RESEARCH ARTICLE

Chimera RNA interference knockdown of γ-synuclein in human cortical astrocytes results in mitotic catastrophe

Timmy Le[1], Cynthia L. Winham[1], Fotis Andromidas[1], Adam C. Silver[1], Evan R. Jellison[2], Aime A. Levesque[1], Andrew O. Koob[1, *]
1 Graduate Program in Neuroscience, Biology Department, University of Hartford, West Hartford, CT, USA
2 Department of Immunology, UCONN Health Center, Farmington, CT, USA

Funding: *This study was supported by grants from the Connecticut Partnership in Innovation and Education (PIE) Fellowship (to TL) and the University of Hartford College of Arts and Sciences Dean's Fund (to TL, FA, AOK).*

Abstract

Elevated levels of γ-synuclein (γ-syn) expression have been noted in the progression of glioblastomas, and also in the cerebrospinal fluid of patients diagnosed with neurodegenerative diseases. γ-Syn can be either internalized from the extracellular milieu or expressed endogenously by human cortical astrocytes. Internalized γ-syn results in increased cellular proliferation, brain derived neurotrophic factor release and astroprotection. However, the function of endogenous γ-syn in primary astrocytes, and the relationship to these two opposing disease states are unknown. γ-Syn is expressed by astrocytes in the human cortex, and to gain a better understanding of the role of endogenous γ-syn, primary human cortical astrocytes were treated with chimera RNA interference (RNAi) targeting γ-syn after release from cell synchronization. Quantitative polymerase chain reaction analysis demonstrated an increase in endogenous γ-syn expression 48 hours after release from cell synchronization, while RNAi reduced γ-syn expression to control levels. Immunocytochemistry of Ki67 and 5-bromodeoxyuridine showed chimera RNAi γ-syn knockdown reduced cellular proliferation at 24 and 48 hours after release from cell synchronization. To further investigate the consequence of γ-syn knockdown on the astrocytic cell cycle, phosphorylated histone H3 pSer10 (pHH3) and phosphorylated cyclin dependent kinase-2 pTyr15 (pCDK2) levels were observed via western blot analysis. The results revealed an elevated expression of pHH3, but not pCDK2, indicating γ-syn knockdown leads to disruption of the cell cycle and chromosomal compaction after 48 hours. Subsequently, flow cytometry with propidium iodide determined that increases in apoptosis coincided with γ-syn knockdown. Therefore, γ-syn exerts its effect to allow normal astrocytic progression through the cell cycle, as evidenced by decreased proliferation marker expression, increased pHH3, and mitotic catastrophe after knockdown. In this study, we demonstrated that the knockdown of γ-syn within primary human cortical astrocytes using chimera RNAi leads to cell cycle disruption and apoptosis, indicating an essential role for γ-syn in regulating normal cell division in astrocytes. Therefore, disruption to γ-syn function would influence astrocytic proliferation, and could be an important contributor to neurological diseases.

***Correspondence to:**
Andrew O. Koob, PhD,
koob@hartford.edu.

orcid:
0000-0003-3381-6770
(Andrew O. Koob)

doi: *10.4103/1673-5374.280329*

Received: *November 25, 2019*
Peer review started: *November 28, 2019*
Accepted: *February 13, 2020*
Published online: *April 3, 2020*

Key Words: *apoptosis; astrocyte; cell cycle; glioblastomas; phospho-histone H3; proliferation; synuclein*

Chinese Library Classification No. *R459.9; R364; R741*

Introduction

The presence of γ-synuclein (γ-syn) has been observed within 63% of high-grade glial tumors, such as glioblastomas and astrocytomas (Fung et al., 2003; El-Agnaf et al., 2007). However, in healthy human tissue, astrocytes in the cortex express γ-syn and retain their ability to successfully reenter the cell cycle to maintain the cellular environment (Little and O'Callagha, 2001; Olsen et al., 2003; Habela et al., 2008; Batista et al., 2014; Dimou and Gotz, 2014). Controlled astrocytic proliferation is likely an important contributor to the neuroenvironment as there is evidence of increased astrocytic proliferation within rodents undergoing operant learning tasks (Rapanelli et al., 2011). Recently, it has been shown that in primary human cortical astrocytes, extracellular γ-syn can be internalized, cause increased cellular proliferation, cell viability and the release of neuroprotective brain derived neurotrophic factor (Winham et al., 2019). Additionally, endogenous γ-syn expression is increased within primary human cortical astrocytes 48 hours after release from cell synchronization (Winham et al., 2019).

Conversely, the increased presence of γ-syn has also been noted within the cerebrospinal fluid of patients with Alzheimer's disease and Dementia with Lewy Bodies (Fung et al., 2003; Oeckl et al., 2016). This finding is of interest because astrocytic γ-syn dysregulation could contribute to abnormal cell cycle re-entry by mature neurons observed in neurodegenerative disease, which leads to cellular arrest and eventually mitotic catastrophe (Goedert, 2001; Hashimoto et al., 2001; Fung et al., 2003; El-Agnaf et al., 2007; Bonda et al., 2010a; Lee et al., 2010; Surgucheva et al., 2014; Oeckl et al., 2016).

It was previously observed that cell cycle progression within advanced stage breast cancer can be hindered through the implementation of lentiviral delivered small interfering RNA (siRNA) (Gu et al., 1992; Ahmad et al., 2007; Satyanarayana and Kaldis, 2009; Ladstein et al., 2010). Under normal conditions, activation of several mitotic regulatory proteins (Mad1, Mad2, Bub1, Bub3, and BubR1) leads to mitotic

arrest in the G2/M-phase of the cell cycle upon mitotic spindle fiber damage (Gupta et al., 2003; Zhu et al., 2014). Out of these mitotic checkpoint proteins, it has been noted in several breast cancer studies that BubR1 is the major protein that γ-syn interacts with in order to override the cell cycle and allow cellular division to progress (Ahmad et al., 2007). Within breast cancer, BubR1 mutations are rare, but it has been documented that γ-syn is able to localize to the poles of mitotic spindle and interact with BubR1 to induce its protein degradation (Ahmad et al., 2007). In addition to protein degradation of BubR1, γ-syn is able to interfere with BubR1 interaction with centromere protein E, a microtubule motor protein, that leads to a disruption in normal mitotic checkpoint signaling (Gupta et al., 2003; Zhu et al., 2014). Therefore, to better understand the role of γ-syn in healthy cells, this study investigated whether γ-syn RNA interference (RNAi) affected astrocytic cellular proliferation and apoptosis in primary astrocytes. In doing so, this could help understand the relationship between γ-syn and astrocytes in neuropathological and healthy tissue.

Materials and Methods

Primary cell culture

Fetal human primary cortical astrocytes (ScienCell, Carlsbad, CA, USA; #1800) were cultured *in vitro* at 37°C with 5% CO_2 in astrocyte medium (ScienCell, #1801) containing 2% fetal bovine serum (ScienCell, #0010), 1% penicillin/streptomycin solution (ScienCell, #0503). Experiments were conducted within 4–5 passages, as per manufacturer's recommendation. Cellular population was allowed to reach 90% confluency before they were passaged and seeded onto poly-l-lysine coated glass coverslips for immunocytochemistry, and 36 mm and 6-well plates for western blot analysis. After seeding at the manufacturer's recommended seeding density, they were allowed to reach 70% confluency in complete media before their cell cycles were synchronized with depleted serum (astrocyte medium, 1% penicillin/streptomycin solution, and 0.25% fetal bovine serum) for 72 hours at 37°C with 5% CO_2. All experiments within this study were conducted with unidentifiable fetal tissue purchased from ScienCell, and in compliance with federal guidelines on the use of fetal tissue for biomedical research. This study was not required to have approval of ethics or human subject research committee, as tissue was unidentifiable.

SNCG chimera RNAi construct

The SNCG chimera RNAi construct was manufactured by Abnova, Taipei, Taiwan, China and distributed by Novus Biologicals (Novus Biologicals, Littleton, CO, USA; #H00006623-R01). The guide strand of the chimeric construct consists of the following 21 nucleic base sequence: 3′ CC AAG GAG AAU GUt gta cag a (1-AS) 5′ while the passenger strand consists of the following sequence: 5′ (1-AA) C UGG UUC CUC UUA CAa cat gt 3′. Within this chimeric construct lower case letters denoted the DNA nucleic base portion of the chimeric RNAi construct while capital letters denoted the RNA nucleic base portion. The mechanism of action of chimera RNAi is initiated through transfection where it associates with dicer which cleaves the double stranded chimera RNAi into a single strand. Afterwards, single-stranded chimera RNAi associates with the RNA-inducing silencing protein complex (RISC) and bind with its target mRNA. The association of the RNAi/RISC complex cleaves the target mRNA into various fragments, which would be degraded by other cellular degradation mechanisms.

To ensure specificity of this commercially available Chimera RNAi construct, the manufacturer applied a sequence design rule devised by Kumiko Ui-Tei that was incapable of inducing off-target effects (Ui-Tei et al., 2004, 2006, 2008). In addition to Ui-Tei's sequence design rule, a mock transfection control was used to put into consideration the possibility of Invitogen® Lipofectamine 2000 (ThermoFisher, Waltham, MA, USA; #11669027) causing unintended effects (Ki et al., 2010).

Treatment conditions

Once the astrocytes' cell cycles were synchronized after the 72 hours depletion period, they were treated with 100 nM of monomeric γ-syn (Abcam, Cambridge, UK; #ab48712), 100 nM of protein control solution (0.1 M sodium chloride, 20 mM Tris-HCl, pH 7.5), 35 nM of RNAi (effective concentration in primary astrocytes) or a vehicle control (1% DEPC water) in complete culture media for 24 or 48 hours before being harvested for western blot analysis or fixated with 4% paraformaldehyde (PFA) in 1× phosphate buffered solution (PBS) for immunocytochemistry. Chimeric RNAi transfection of human cortical astrocytes was accomplished by using 5 μL of Invitogen® Lipofectamine 2000 (ThermoFisher, #11669027) per 2.8 μmol of chimera RNAi as recommended by the manufacturer.

Quantitative polymerase chain reaction

RNA from Time 0, vehicle control and 35 nM RNAi treated human cortical astrocytes were isolated using the RNeasy Mini kit (Qiagen, Hilden, Germany) in conjunction with the RNase-Free DNase Set (Qiagen). cDNA was synthesized using the high capacity cDNA reverse transcription kit according to manufacturer's instructions (ThermoFisher). Relative quantitation of mRNA levels was performed by quantitative PCR via TaqMan Gene Expression Assays (ThermoFisher) and TaqMan Gene Expression Master Mix (ThermoFisher) using a StepOnePlus (ThermoFisher) system. Analyses were performed using the standard curve method with β-actin as the normalizing endogenous control. Relative quantitative values were determined by dividing the relative quantity for the target gene by the relative quantity for β-actin. *Actb* Hs01060665_g1 and *Sncg* Hs00268306_m1 TaqMan Gene Expression Assays (ThermoFisher) were used.

Western blot analysis

Samples for synchronized western blot analysis at 24 and 48 hours were harvested from their respective plates by two quick washes with 1× PBS. Afterwards, the cells were lysed with 50 μL of lysis buffer (20 mM TrisHCl, 150 mM NaCl, 1 mM EDTA, 0.5% NP40, 2 mM 2-mercaptoethanol, 1× protease and phosphatase inhibitors, pH 7.4) through a 40 minutes incubation period at 4°C. Later the cells were scraped from their plates, collected, sonicated, and stored at (–80°C)

for western blot analysis.

Total protein concentration of whole cell lysate from each sample was determined using Pierce® BCA protein assay kit (ThermoScientific, Waltham, MA, USA; #23225). 20 μL of each sample was loaded and separated on 4–12% Bis-Tris gels (Invitrogen, Carlsbad, CA, USA; #NP0321) and the proteins was electrotransferred onto 0.2 μm PVDF membranes (BioRad, Hercules, CA, USA; #1620174) using 1× 3-[Cyclohexylamino]-1-propaneosulfonic acid (CAPS) buffer containing 20% methanol. Membranes were blocked using 3% milk in 1× PBS with 0.1% Triton-X 100 (PBS-T) for an hour and then incubated overnight in polyclonal rabbit antibodies diluted in 3% bovine serum albumin (BSA) (Sigma, Kawasaki, Japan; #A2058) in PBS-T at 4°C. The following polyclonal rabbit antibodies were used: anti-γ-syn (1:2000) (ThermoFisher, #PA5-29142) and a cell cycle cocktail (1:250) (Abcam, #ab136810) that targets phosphorylated cyclin-dependent kinase-2 pTyr15 (pCdk2), phosphorylated histone H3 pSer10 (pHH3), and β-actin. Membranes were then incubated in goat anti-rabbit IgG secondary antibody conjugated to horseradish peroxidase (1:2000; American Qualex, #A102PN) in PBS-T and 3% BSA for 1 hour at ambient conditions. Visualization of protein expression levels was achieved by the use of enhanced chemilunescence (ECL) (PerkinElmer, #NEL120001EA), and photographed with GENEGnome (Syngene Bio Imaging, Bangalore, India). Quantification of protein expression levels was obtained with the use of the ImageJ software (https://imagej.nih.gov/ij/, public domain, BSD-2). Background noise was removed; the bands of the protein of interest were then quantified by dividing the protein of interest's pixel density to its respective actin pixel density.

Immunocytochemistry

After the 72 hour depletion period, the cells were subjected to a 35 nM RNAi transfection or a vehicle control (1% DEPC water) in complete culture media with 10 μM 5-bromodeoxyuridine (BrdU) (BD Pharmingen, San Jose, CA, USA; #550891) for 24 or 48 hours. Chimera RNAi transfection of human cortical astrocytes was accomplished using Invitogen® Lipofectamine 2000. After which, the coverslips were fixed with 4% paraformaldehyde (PFA) in 1× PBS for 20 minutes at 4°C and then stored in 1× PBS at 4°C until fluorescent labeling.

Immunocytochemistry staining was accomplished by washing previously fixed coverslip in 1 × PBS 3 × 5 minutes and then permeabilized with 0.3% Triton-X 100 and 10% goat serum (Vector, Burlingame, CA, USA; #S-1000) in 1× PBS for 1 hour at ambient conditions to block non-specific antibody binding. Afterwards, coverslips were labeled with rabbit anti-Ki67 antibodies (1:50; Novus Biologicals, Littleton, CO, USA; #NB600-1252) in 1× PBS at 4°C overnight. Later, coverslips were washed in 1× PBS 3 × 5 minutes and then incubated at ambient conditions in the dark for 2 hours with DyLight® 594 anti-rabbit IgG secondary antibody (1:200; Vector, #DI-1549) in 0.3% Triton-X 100 in 1× PBS (0.3% PBS-T). Coverslips were then washed 3 × 5 minutes with 1× PBS, fixed with 4% PFA in 1× PBS for 10 minutes at ambient conditions, followed by 3 × 5 minutes 1× PBS washes. BrdU labeling was initiated by incubating coverslips for 15 minutes in 2 N HCl at ambient conditions, followed by a 15-minute incubation period at 37°C and 5% CO_2. Afterwards, coverslips were quickly rinsed and then incubated at ambient conditions for 10 minutes with boric acid (pH 8.5). Coverslips were then washed with 1× PBS 3 × 5 minutes and blocked with 10% goat serum in 0.3% PBS-T for 1 hour at ambient conditions. After blocking treatment, coverslips were labeled with rat primary BrdU antibody (1:500; Novus Biologicals, #NB500-169) in 0.03% 1× PBS-T at 4°C overnight. Coverslips were then washed 3 × 5 minutes with 1× PBS and then labeled with Invitogen® Alexa Fluor® 488 anti-rat IgG secondary antibody (1:400; ThermoFisher, A11006). Finally, coverslips were washed with a final round of 1× PBS 3 × 5 minutes, mounted on slides, and counterstained for cellular nuclear labeling with 4′,6-diamidino-2-phenylindole (DAPI; vectastain, Vector).

Stereology

Unbiased stereological analyses of Ki67, BrdU, and DAPI labeled cells was performed on Axiostar plus fluorescent microscope, Zeiss, Oberkochen, Germany by randomly choosing four 2.7×10^5 μm^2 fields from each experimental condition blinded coverslip. In addition, three fields from each of the four coverslips were taken in order to produce a sample size of 12. Total cell count was performed and evaluated for each condition in regard to fluorescent co-localization to determine proliferation, exiting, and non-proliferation rate of each condition. Proliferation rate was determined by the co-localization of Ki67 and BrdU over the total number of DAPI positive cells. Non-proliferation rate is determined by astrocytes that were not positive for either Ki67 or BrdU proliferative markers, therefore cells that were only DAPI positive were considered to be non-proliferative. Exiting rate was defined as cells that were exiting the cell cycle and was quantified by analyzing cells that were only positive for BrdU and not Ki67 over the total DAPI positive cells.

Flow cytometry

After cell cycle arrest via serum starvation, samples from 6-well cell culture plates were treated in quadruplicates with 35 nM of RNAi or a vehicle control in complete astrocyte culture media for 24 or 48 hours. After the completion of treatment at the respective time points, cells were harvested, suspended in 70% ethanol for fixation, and stored at –80°C for flow cytometry analysis.

Flow cytometry cell labeling was accomplished by first thawing fixed cells and removing the 70% ethanol fixative via centrifugation at 376 × *g*/4°C for 10 minutes. The cell pellet was resuspended in wash buffer (1× PBS) and the wash buffer was removed via centrifugation at 376 × *g*/4°C for 10 minutes. Cellular DNA content was labeled with propidium iodide (PI) solution (0.1 mg/mL) and RNAse-A (1 mg/mL) in 1× PBS. Cells were then stored in the dark on wet ice until analysis (< 1 hour).

Flow cytometry to quantify the total DNA content of the cells by PI was performed using MACSQuant® Analyzer (MiltenyiBiotec, Somerville, MA, USA) with fluorescence excitation at 488 nM and emission collected at 655–730 nm.

Flow cytometry data analysis was performed using FlowJo software (version 10.5.3; Tree Star, Ashland, OR, USA).

Statistical analyses

Statistical significance within this study was determined by using an unpaired *t*-test with the exception of the quantitative polymerase chain reaction (qPCR) results which used a one-way analysis of variance (ANOVA) with Dunnett's *post-hoc* test. The results from both statistical methodologies were considered to be statistically significance if the *P*-value is less than 0.05.

Results

Knockdown of γ-syn and protein expression

After cell synchronization with serum depletion, human cortical astrocytes were treated with γ-syn RNAi when serum was reintroduced, and cells were released back into the cell cycle. In **Figure 1A**, a timeline delineates the experimental conditions. qPCR data (**Figure 1B**) shows relative γ-syn mRNA expression over the course of 48 hours after release from cell synchronization. Comparison of the vehicle control data gathered from the 24 and 48 hours indicated a higher level of relative γ-syn mRNA level at 48 hours than at 24 hours ($P < 0.05$). In addition, the knockdown effect of chimera RNAi was not seen at 24 hours but rather at 48 hours relative to their respective vehicle controls ($P < 0.05$). Coinciding with the qPCR knockdown results, western blot analysis of γ-syn (**Figure 2A**) revealed no significant knockdown effect on the endogenous γ-syn protein expression at 24 hours (**Figure 2B**), but a significant decrease at 48 hours ($P < 0.05$) relative to the respective vehicle controls at each time point.

Effects of chimera RNAi mediated knockdown of γ-syn on the astrocytic cell cycle

To investigate the initial effects of RNAi mediated knockdown of γ-syn on the astrocytic cell cycle, immunocytochemistry analysis with BrdU and Ki67 proliferation markers was employed. BrdU was added during serum reintroduction. At 24 hours after release from cell cycle synchronization, there was a decrease in both Ki67 and BrdU positive cells in the RNAi condition relative to the vehicle control ($P < 0.01$ and $P < 0.05$; **Figure 3B**). Ki67 and BrdU colocalization showed no significant differences in the proliferation rate at 24 hours (**Figure 3A** and **B**). Furthermore, assessment of the exiting rate as determined BrdU positive cells with no colocalization with Ki67, also showed no significant difference between the RNAi condition and the vehicle control (**Figure 3A** and **B**). Likewise, analysis of DAPI blue positive cells without any colocalization with Ki67 and BrdU resulted in no significant difference in the non-proliferation rate. When the same criteria were applied at 48 hours, immunocytochemistry results show a decrease in both Ki67 and BrdU positive cells in the RNAi condition relative to the vehicle control (**Figure 4A**; $P < 0.01$ and $P < 0.05$). Contrary to what was observed at 24 hours, there was a decrease in the proliferation rate within the RNAi condition relative to the vehicle control (**Figure 4B**; $P < 0.05$). Additionally, there was an increase in the cell cycle exiting rate as well as the non-proliferative rate within the RNAi transfected cells in comparison to cells that were not transfected with RNAi ($P < 0.01$).

Cell cycle regulatory protein

Western blot analysis for pHH3 and pCDK2 was also applied to further understand the effects of γ-syn on the astrocytic cell cycle. Specifically, it was of interest to understand the effects on the cell cycle regulatory protein at M-phase (pHH3) and G2/S (pCDK2). Treatment of 100 nM of extracellular monomeric recombinant γ-syn (**Figure 5G**) demonstrated a decrease in astrocytic pHH3 protein expression ($P < 0.05$) at 24 hours (**Figure 5C**) within the γ-syn treatment condition relative to the control. However, this effect dissipated at 48 hours (**Figure 5F**) with no significant differences between the extracellular γ-syn treatment condition and control. In addition, no significant differences were observed at either 24 or 48 hours when probed with pCDK2 (**Figure 5B** and **E**).

When endogenous γ-syn expression was knocked down with chimera RNAi, the reverse effect was seen and coincided with decreased γ-syn expression at 48 hours (**Figure 6**). There were no significant differences in either the pHH3 and pCDK2 protein expression levels amongst the RNAi condition and vehicle control at 24 hours post release from cell synchronization (**Figure 6B** and **C**). pHH3 protein expression was increased within the RNAi condition relative to the vehicle control at 48 hours ($P < 0.01$; **Figure 6F**). Additionally, there were no difference between the RNAi condition and the vehicle control for pCDK2 at 48 hours (**Figure 6E**).

Mitotic catastrophe as a result of chimera RNAi mediated knockdown of γ-syn

To determine if chromosome condensation as a result of increased pHH3 caused G_2/M phase cellular arrest, synchronized astrocytes were treated with PI and analyzed via flow cytometry (**Figure 7**). Interestingly, G_2/M phase was noticeably lower in RNAi treated cells when comparing 24 and 48 hours, and also in comparison to the vehicle control at 48 hoursThe stages of the cell cycle were then further assessed via flow cytometry after PI treatment (**Figure 8**), which revealed an increase in G_1/G_0 frequency within the vehicle control at 48 hours relative to 24 hours ($P < 0.05$; **Figure 8B**). G_2/M frequency showed increases in the vehicle control at 24 hours relative to Time 0 ($P < 0.05$; **Figure 8C**), but no significant change was observed between 24 and 48 hours in the vehicle control. When the RNAi condition was examined, a decrease in G_2/M frequency at 48 hours relative to 24 hours was confirmed ($P < 0.01$) (**Figure 8C**). S frequency analysis showed an increase at 24 hours ($P < 0.01$) within both vehicle control and RNAi condition relative to Time 0 (**Figure 8D**). However, when the S frequency was compared between 24 and 48 hours, there was a decrease at 48 hours within both the vehicle control and RNAi transfected condition ($P < 0.01$).

The results indicate a qualitative shift toward the sub-2N population of cells, indicative of an increase in apoptotic frequency within the RNAi condition in comparison to Time 0, control, and vehicle control at 48 hours, but not at 24 hours (**Figure 8A**). Therefore, the results indicate that as chromosomes condensed, as evidenced by increased pHH3, the cells

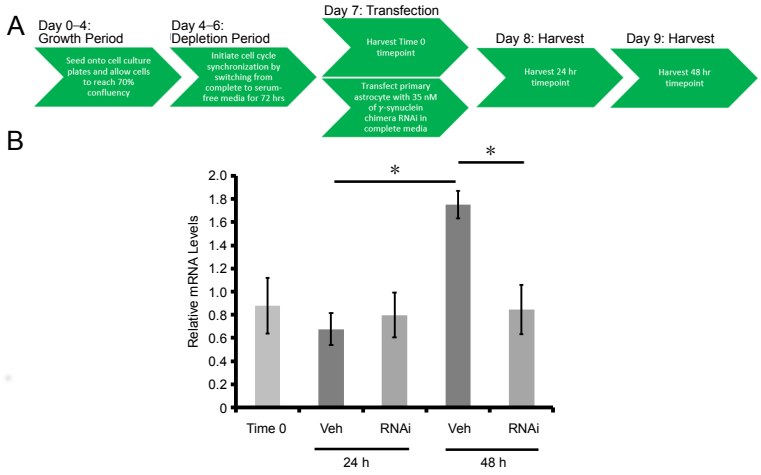

Figure 1 Relative γ-synuclein mRNA levels.
(A) Timeline of human cortical astrocyte cell cycle synchronization, and subsequent γ-synuclein RNA interference treatment with serum reintroduction. (B) Relative γ-synuclein mRNA levels were measured using quantitative polymerase chain reaction and compared with β-actin of each respective sample. At 24 hours, there were no significant results between the four treatment conditions. However, at 48 hours, there was significant decrease in relative mRNA level in astrocytes that were transfected with chimera RNA interference in comparison to the other three treatment conditions. Bar graph shows the mean ± SEM, n = 3 or 4 (*P < 0.05; one-way analysis of variance followed by Dunnet's *post-hoc* test). Veh: Venicle control.

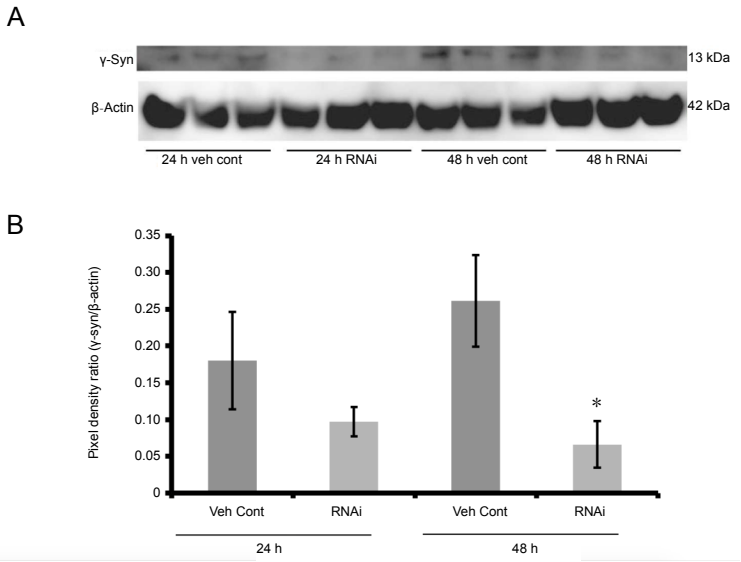

Figure 2 Knockdown of γ-syn protein expression with chimera RNAi transfection of human cortical astrocytes.
(A) Immunoblot with primary antibodies directed towards γ-syn (13 kDa) within vehicle control (Veh Cont) and 35 nM chimera RNAi treated samples at 24 and 48 hours. (B) Quantification of the protein expression levels performed by comparing the pixel density ratio of γ-syn to its respective β-actin expression level in each of the conditions. The results show no significant change at 24 hours, but a significant decrease in γ-syn protein expression levels at 48 hours within the chimera RNAi treated condition in comparison to the vehicle control. Bar graph shows the mean ± SEM, n = 3 (*P < 0.05; unpaired t-test). RNAi: RNA interference; γ-syn: γ-synuclein.

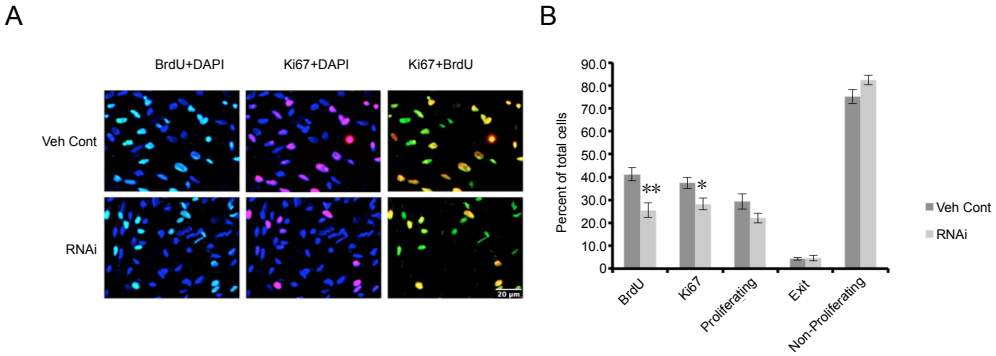

Figure 3 Immunocytochemistry stereological analysis of Ki67, BrdU, and DAPI at 24 hours after release from cell cycle synchronization.
(A) Representative fields of treated cells labeled with BrdU (green), Ki67 (orange), and DAPI (blue). Images also contained merged images of BrdU + DAPI (turquoise) and Ki67 + DAPI (magenta). Scale bar: 20 μm. (B) Bar graph shows frequency of cells expressing BrdU, Ki67, or BrdU + Ki67 in the vehicle control (Veh Cont) and RNAi treated condition. Analysis show decrease in the frequency of BrdU positive cells within RNAi when compared with control. Furthermore, frequency of Ki67 cells is decreased when compared with the vehicle control. No significance was observed in regard to proliferative cells (Ki67 + BrdU colocalized cells), exiting (BrdU positive without colocalization), and non-proliferative rate (DAPI positive without colocalization). Three fields from each of the four coverslips were taken in order to produce a sample size of 12 (n = 12). Bar graph shows the mean ± SEM (*P < 0.05; **P < 0.01; unpaired t-test). BrdU: 5-Bromodeoxyuridine; DAPI: 4′,6-diamidino-2-phenylindole; RNAi: RNA interference.

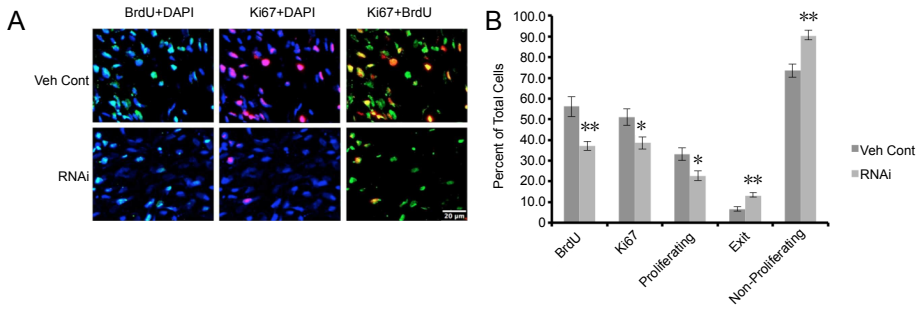

Figure 4 Immunocytochemistry stereological analysis of Ki67, BrdU, and DAPI at 48 hours after release from cell cycle synchronization.
(A) Representative fields of treated cells labeled with BrdU (green), Ki67 (orange), and DAPI (blue). Images also contained merged images of BrdU + DAPI (turquoise) and Ki67 + DAPI (magenta). Scale bar: 20μm. (B) Bar graph shows frequency of cells expressing BrdU, Ki67, or BrdU + Ki67 in the vehicle control (Veh Cont) and RNAi condition. A decrease in the frequency of BrdU positive cells was observed in the RNAi condition relative to the vehicle control. Additionally, there were less Ki67 positive cells as well as proliferative cells (Ki67 + BrdU colocalized cells) in the RNAi condition when compared with the vehicle control. The RNAi condition also showed an increase in cells exiting the cell cycle (BrdU positive without colocalization) as well as non-proliferative cells (DAPI positive without colocalization)) when compared with vehicle control. Three fields from each of the four coverslips were taken to produce a sample size of 12 (n = 12). Bar graph shows the mean ± SEM (*P < 0.05; **P < 0.01; unpaired t-test). BrdU: 5-Bromodeoxyuridine; DAPI: 4′,6-diamidino-2-phenylindole; RNAi: RNA interference.

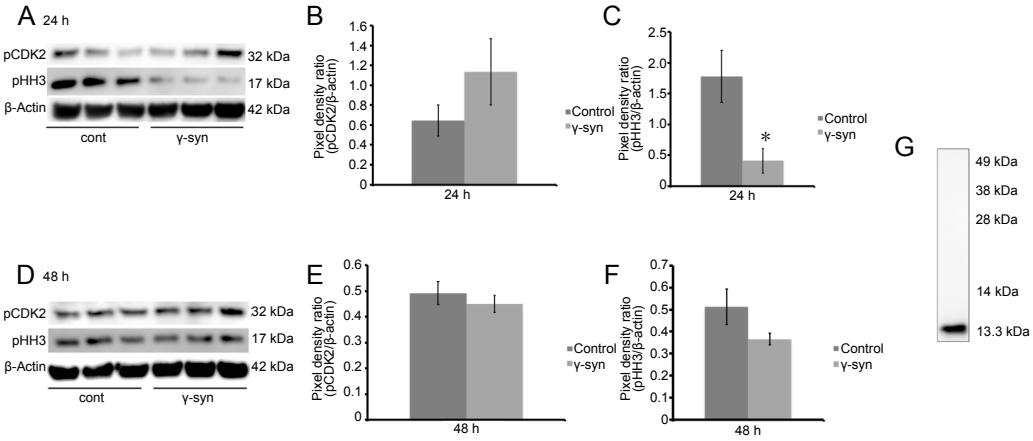

Figure 5 The effects of extracellular γ-syn on the astrocytic cell cycle.
(A) Immunoblot with primary pCDK2 (32 kDa) and pHH3 (17 kDa) antibodies directed towards γ-syn treated cell at 24 hours. Quantification via pixel density ratio of pCDK2 (B) and pHH3 (C) with its respective actin (42 kDa) at 24 hours show a decrease in pHH3 expression in the γ-syn treated condition relative to the control while no significance in the pCDK2 blot. (D) Immunoblot with primary pCDK2 and pHH3 antibodies directed towards γ-syn treated cells at 48 hours. Immunoblot quantification via pixel density ratio of pCDK2 (E) and pHH3 (F) with its respective actin at 48 hours shows no significant difference between the γ-syn treated condition relative to the control. (G) Immunoblot of monomeric γ-syn (13.3 kDa) preparation used in this study, with no observed dimerization (28 kDa), and without trimers or tetramers near higher ladder bands at 38 or 49 kDa. Bar graph shows the mean ± SEM, n = 3 (*P < 0.05; unpaired t-test). Protein normalization was determined via BCA Assay. pCDK2: Phosphorylated cyclin dependent kinase-2 pTyr15; pHH3: phosphorylated histone H3 pSer10; RNAi: RNA interference; γ-syn: γ-synuclein.

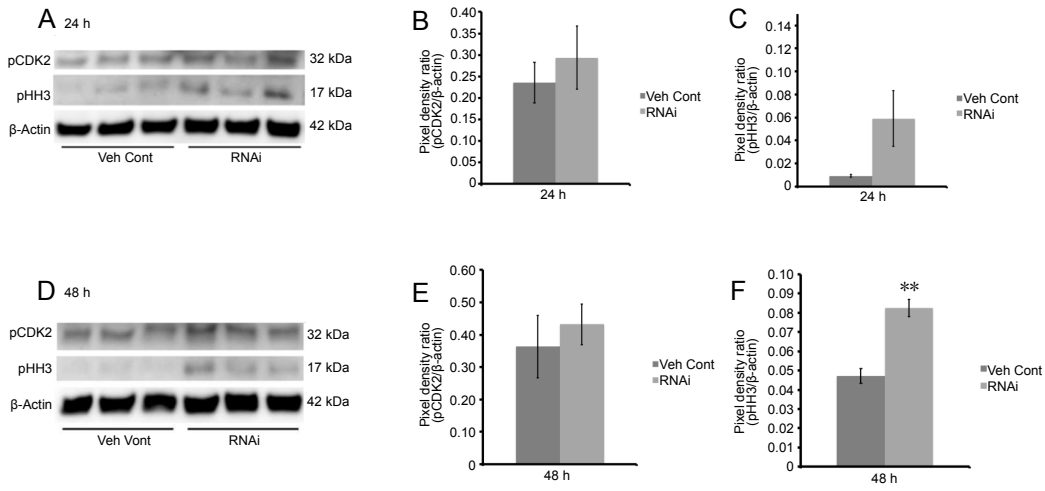

Figure 6 pCDK2, and pHH3 protein expression levels in RNAi transfected cells after release from cell cycle synchronization.
(A) Immunoblots of whole human cortical astrocytes lysate with primary antibodies directed towards pCDK2 (32 kDa) and pHH3 (17 kDa) at 24 hours post release from cell synchronization show no significance in pCDK2 (B) or pHH3 (C) protein expression levels when compared with the vehicle control. (D) Immunoblots of whole human cortical astrocytes lysate with primary antibodies directed towards pCDK2 (32 kDa) and pHH3 (17 kDa) at 48 hours post release from cell synchronization show no significant difference in (E) pCDK2 levels, but a significant increase in (F) pHH3 protein expression in the RNAi condition relative to the vehicle control. Bar graph shows the mean ± SEM, n = 3 (*P < 0.05; **P < 0.01; unpaired t-test). Protein normalization was determined via BCA Assay. pCDK2: Phosphorylated cyclin dependent kinase-2 pTyr15; pHH3: phosphorylated histone H3 pSer10; RNAi: RNA interference.

were unable to survive and mitotic catastrophe ensued. Additionally, there was an increase in the apoptotic frequency within the RNAi condition at 48 hours relative to 24 hours ($P < 0.05$; **Figure 8E**) while there was no significant difference within the vehicle controls.

Discussion

γ-Syn was first identified as Breast Cancer Specific Gene-1 in mammals due to its high expression levels within breast cancer when compared to non-cancerous cells (Jia et al., 1999; Surgucheva and Surguchov, 2008; He et al., 2018). Specifically, γ-syn contributes to breast and ovarian tumor motility and invasion as well as their cellular survival by allowing these tumorous cells to be more resilient towards chemotherapeutic drugs than their cancer naïve counterparts (Wu et al., 2003; Zhu et al., 2014). The main quality that allows γ-syn to exert its effects within these types of tumors is its ability to compromise the spindle assembly checkpoint (Zhu et al., 2014).

Furthermore, it has been noted that γ-syn overexpression, as seen in advanced stage cancer, can suppress the activities of caspase-3 and caspase-9, leading to the prevention of cellular apoptotic function that results from BubR1 activity (Pan et al., 2002). γ-Syn can therefore override G2/M-phase cellular arrest by degrading or interfering with BubR1 as well as suppressing caspase activities. This allows tumorous cells to continue cellular proliferation unobstructed by any cellular regulation. On the contrary, other breast cancer studies have demonstrated that γ-syn mediated breast cancer proliferation can be inhibited by knocking down the expression of γ-syn with the implementation of lentiviral delivered siRNA (He et al., 2018).

Therefore, as human cortical astrocytes are expressing γ-syn within non-pathological conditions this could possibly provide a mechanism to exhibit its proliferative abilities in order to progress normally through the cell cycle (Guizzetti et al., 2011; Ge and Jia, 2016). When relative mRNA levels were measured within the γ-syn RNAi conditions, a noticeable decrease was observed at the gene and protein levels. In conjunction with γ-syn knockdown, a decrease in cellular proliferation and increase in apoptosis occurred, supporting previous results that indicate γ-syn expression could be astroprotective in addition to supporting progression through the cell cycle (Cooper, 2005; McDonough and Martínez-Cerdeño, 2012; Winham et al., 2019).

Therefore, the data suggests that chimera RNAi exhibits its inhibiting effects on astrocytic proliferation. Additionally, BrdU and Ki67 immunocytochemistry revealed that proliferation inhibition subsequently leads to an increase in the cell cycle exiting rate at 48 hours (Siegenthaler and Miller, 2005). However, BrdU and Ki67 immunocytochemistry results are inconclusive in regard to cell death, or when the cells absquatulate the cell cycle, as it is possible to exit from any particular phase of the cell cycle (Hitomi and Stacey, 1999; Spencer et al., 2013).

Western blot analysis with antibodies directed towards pHH3 and pCDK2, which are proteins that regulate the M-phase and G1/S-phase of cell cycle respectively pinpointed the effect of γ-syn likely on M-phase progression, with γ-syn knockdown resulting in increased pHH3 expression, and also coinciding with previous results in other cell lines (Pucci et al., 2000; Welburn et al., 2007; Luo et al., 2010).

Likewise, it was previously reported that extracellular γ-syn was able to induce cellular proliferation in human cortical astrocytes at 24 hours after release from synchronization (Winham et al., 2019). A decrease in pHH3 expression in γ-syn treated astrocytes occurred at 24 hours, but not at 48 hours, coinciding with γ-syn treatment induced proliferation time points. The initial proliferation period of cultured astrocytes is approximately 16–24 hours after growth serum reintroduction and it is possible that endogenous astrocytic γ-syn is interacting with BubR1 during this time point (Gupta et al., 2003; Zhu et al., 2014; Winham et al., 2019). Furthermore, there was no significant difference in regards to pCDK2 expression at either 24 and 48 hours corroborating previous data that γ-syn has a greater effect at the M-phase of the astrocytic cell cycle (Gupta et al., 2003). In addition, pHH3 protein expression was not significant at 48 hours relative to its respective control, indicting the effect of γ-syn protein treatment occurs during initial cellular division. Likewise, after 48 hours, although the effect on pHH3 is no longer observed, it was shown that there was a subsequent increase in cellular viability, as well as increased expression and release of brain-derived neurotrophic factor (Winham et al., 2019).

In relation to neurodegenerative diseases, the ultimate fate of cells that are arrested within the cell cycle and cannot complete proliferation is mitotic catastrophe (Nagy et al., 1997). Therefore, it was of interest to investigate the consequence of astrocytic cell cycle arrest and determine if cells remained in arrest, or if they undergo mitotic catastrophe similar to M-phase arrested neurons and other cell types (Bonda et al., 2010b; Orth et al., 2012; Xia et al., 2015). When cells were analyzed via flow cytometry after PI treatment, the shift in sub-2N cells confirmed that the result was mitotic catastrophe.

Therefore, the studies here provide initial evidence of mitotic catastrophe induced by γ-syn knockdown. Although 35 nM was the effective concentration of γ-syn chimera RNAi induced gene silencing, based previous studies of chimera RNAi and siRNA transfection within astrocytes (Ui-Tei et al., 2008; Ki et al., 2010), a dilution series to determine the onset of apoptosis would be beneficial (Ui-Tei et al., 2008; Caffrey et al., 2011). This could be conducted with further studies on levels of cleaved caspase-3 or Annexin V in conjuction with PI in unpermeabilized cells, which would further characterize and confirm the apoptotic events observed here in a temporal and concentration dependent manner (Slee et al., 2001; Pan et al., 2002; Rieger et al., 2011; Poskanzer and Yuste, 2016). Even though PI labeling for sub-2n analysis allows for an accurate approximation of apoptotic events, it is possible that there are some necrotic events as well since PI readily labels cells that have compromised cellular membrane (Riccardi and Nicoletti, 2006). However, the results of γ-syn RNAi induced apoptosis clearly coincide with expression knockdown at 48 hours, and there were no

differences in sub-2n/apoptotic events between 24 and 48 h within the vehicle control.

In conclusion, the results of this study allow for a greater understanding of the function of γ-syn on the astrocytic cell cycle in normal states, and the possible consequence of disrupting this mechanism of action. Namely, if astrocytes are not capable of proliferation due to γ-syn dysfunction, then CNS pathology can ensue due to a lack of regulation within the brain parenchyma (Winham et al., 2019). Such pathology could be neurodegenerative diseases which is associated with synaptic loss and changes, and disruption to the astrocytic cell cycle that could cause atrophy and subsequently lead to catastrophic effects on the synapse (Pekny et al., 2016). In addition to understanding the role of astrocytes within neurodegenerative diseases, findings from this study could potentially lead to RNA therapy to minimize cancer neovascularization and growth due to the overexpression of γ-syn. Knocking down γ-syn mediated breast cancer cellular proliferation with a lentiviral delivered siRNA reduced tumor size, and future studies involving the knockdown of γ-syn within glioma cell lines could open up new avenues in cancer research (Mello and Conte, 2004; He et al., 2018).

Acknowledgments: *Special thanks to Brooke MacKinnon and Melanie Shaffer, The University of Hartford, in assisting with tissue culture maintenance and harvesting, and to Irene Luccia Pearl for help with manuscript preparation. Further support was provided by the University of Hartford M.S. Neuroscience Program.*
Author contributions: *Study design: TL, CLW, AOK; experimental implementation: TL, CLW, FA, ACS, AAL; data collection: TL, ACS, ERJ; data analysis: TL, ACS, ERJ, AOK; paper writing: TL, AOK. All authors approved the final version of the paper.*
Conflicts of interest: *The authors of this manuscript declare that they do not have any conflict of interest.*
Financial support: *Funding was provided by the Connecticut Partnership in Innovation and Education (PIE) Fellowship (to TL) and the University of Hartford College of Arts and Sciences Dean's Fund (to TL, FA, AOK).*
Institutional review board statement: *This study was not required to have approval of ethics or human subject research committee, as tissue was unidentifiable.*

Data sharing statement: *Datasets analyzed during the current study are available from the corresponding author on reasonable request.*
Plagiarism check: *Checked twice by iThenticate.*
Peer review: *Externally peer reviewed.*

Open peer reviewers: *Luciana P. Cartarozzi, University of Campinas (UNICAMP), Brazil; Ana-Maria Buga, University of Medicine and Pharmacy of Craiova, Romania.*
Additional file: *Open peer review report 1.*

References

Ahmad M, Attoub S, Singh MN, Martin FL, El-Agnaf OM (2007) Gamma-synuclein and the progression of cancer. FASEB J 21:3419-3430.
Batista CM, Mariano ED, Barbosa BJ, Morgalla M, Marie SK, Teixeira MJ, Lepski G (2014) Adult neurogenesis and glial oncogenesis: when the process fails. Biomed Res Int 2014:438639.
Bonda DJ1, Bajić VP, Spremo-Potparevic B, Casadesus G, Zhu X, Smith MA, Lee HG (2010a) Review: cell cycle aberrations and neurodegeneration. Neuropathol Appl Neurobiol 36:157-163.
Bonda DJ, Lee HP, Kudo W, Zhu X, Smith MA, Lee HG (2010b) Pathological implications of cell cycle re-entry in Alzheimer disease. Expert Rev Mol Med 12:e19.
Caffrey DR, Zhao J, Song Z, Schaffer ME, Haney SA, Subramanian RR, Seymour AB, Hughes JD (2011) siRNA off-target effects can be reduced at concentrations that match their individual potency. PLoS One 6:e21503.
Cooper S (2005) Reanalysis of the protocol for in vitro synchronization of mammalian astrocytic cultures by serum deprivation. Brain Res Brain Res Protoc 15:115-118.
Dimou L, Gotz M (2014) Glial cells as progenitors and stem cells: new roles in the healthy and diseased brain. Physiol Rev 94:709-737.
Fung KM, Rorke LB, Giasson B, Lee VM, Trojanowski JQ (2003) Expression of Alpha-, Beta-, and Gamma-synuclein in glial tumors and medulloblastomas. Acta Neuropathol 106:167-175.
Ge WP, Jia JM (2016) Local production of astrocytes in the cerebral cortex. Neuroscience 323:3-9.
Goedert M (2001) Alpha-synuclein and neurodegenerative diseases. Nat Rev Neurosci 2:492-501.
Gu Y, Rosenblatt J, Morgan DO (1992) Cell cycle regulation of CDK2 activity by phosphorylation of Thr160 and Tyr15. EMBO J 11:3995-4005.
Guizzetti M, Kavanagh TJ, Costa LG (2011) Measurements of astrocyte proliferation. In: Methods in molecular biology (Clifton NJ, ed), pp 349–359. Totowa, NJ: Humana Press.
Gupta A, Inaba S, Wong OK, Fang G, Liu J (2003) Breast cancer-specific gene 1 interacts with the mitotic checkpoint kinase BubR1. Oncogene 22:7593-7599.
Habela CW, Olsen ML, Sontheimer H (2008) ClC3 is a critical regulator of the cell cycle in normal and malignant glial cells. J Neurosci 28:9205-9217.
Hashimoto M, Rockenstein E, Mante M, Mallory M, Masliah E (2001) beta-Synuclein inhibits alpha-synuclein aggregation: a possible role as an anti-parkinsonian factor. Neuron 32:213-223.
He JS, Xie N, Yang JB, Guan H, Chen WC, Zou C, Ouyang YW, Mao YS, Luo XY, Pan Y, Fu L (2018) BCSG1 siRNA delivered by lentiviral vector suppressed proliferation and migration of MDA-MB-231 cells. Int J Mol Med 41:1659-1664.
Hitomi M, Stacey DW (1999) Cellular ras and cyclin D1 are required during different cell cycle periods in cycling NIH 3T3 cells. Mol Cell Biol 19:4623-4632.
Jia T, Liu YE, Liu J, Shi YE (1999) Stimulation of breast cancer invasion and metastasis by synuclein γ1. Cancer Res 59:742-747.
Ki KH, Park DY, Lee SH, Kim NY, Choi BM, Noh GJ (2010) The optimal concentration of siRNA for gene silencing in primary cultured astrocytes and microglial cells of rats. Korean J Anesthesiol 59:403-410.
Ladstein RG, Bachmann IM, Straume O, Akslen LA (2010) Ki-67 expression is superior to mitotic count and novel proliferation markers PHH3, MCM4 and mitosin as a prognostic factor in thick cutaneous melanoma. BMC Cancer 10:140.
Lee HJ, Suk JE, Patrick C, Bae EJ, Cho JH, Rho S, Hwang D, Masliah E, Lee SJ (2010) Direct transfer of α-synuclein from neuron to astroglia causes inflammatory responses in synucleinopathies. J Biol Chem 285:9262-9272.
Little AR, O'Callagha JP (2001) Astrogliosis in the adult and developing CNS: is there a role for proinflammatory cytokines? Neurotoxicology 22:607-618.
Luo J, Xu X, Hall H, Hyland EM, Boeke JD, Hazbun T, Kuo M-H (2010) Histone h3 exerts a key function in mitotic checkpoint control. Mol Cell Biol 30:537-549.
McDonough A, Martínez-Cerdeño V (2012) Endogenous proliferation after spinal cord injury in animal models. Stem Cells Int 2012:387513.
Mello CC, Conte D (2004) Revealing the world of RNA interference. Nature 431:338-342.
Nagy Z, Esiri MM, Smith AD (1997) Expression of cell division markers in the hippocampus in Alzheimer's disease and other nenrodegenerative conditions. Acta Neuropathol 93:294-300.
Oeckl P, Metzger F, Nagl M, von Arnim CAF, Halbgebauer S, Steinacker P, Ludolph AC, Otto M (2016) Alpha-, beta-, and gamma-synuclein quantification in cerebrospinal fluid by multiple reaction monitoring reveals increased concentrations in Alzheimer's and Creutzfeldt-Jakob disease but no alteration in synucleinopathies. Mol Cell Proteomics 15:3126-3138.
Olsen ML, Schade S, Lyons SA, Amaral MD, Sontheimer H (2003) Expression of voltage-gated chloride channels in human glioma cells. J Neurosci 23:5572-5582.
Orth JD, Loewer A, Lahav G, Mitchison TJ (2012) Prolonged mitotic arrest triggers partial activation of apoptosis, resulting in DNA damage and p53 induction. Mol Biol Cell 23:567-576.
Pan ZZ, Bruening W, Giasson BI, Lee VM, Godwin AK (2002) γ-synuclein promotes cancer cell survival and inhibits stress- and chemotherapy drug-induced apoptosis by modulating MAPK pathways. J Biol Chem 277:35050-35060.
Pekny M, Pekna M, Messing A, Steinhäuser C, Lee JM, Parpura V, Hol EM, Sofroniew MV, Verkhratsky A (2016) Astrocytes: a central element in neurological diseases. Acta Neuropathol 131:323-345.
Poskanzer KE, Yuste R (2016) Astrocytes regulate cortical state switching in vivo. Proc Natl Acad Sci U S A 113:E2675-2684.

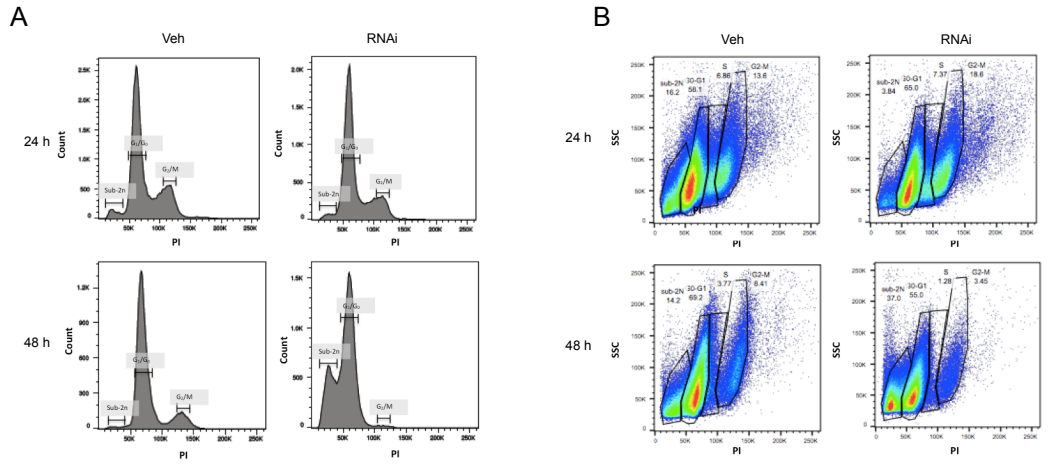

Figure 7 Propidium iodide labeled astrocytes analyzed via flow cytometry.
Representative histogram (A) and concatenated dot-plots (B) of propidium iodide labeled human cortical astrocytes data show human cortical astrocytes at a specific phase of the cell cycle as well as sub-2n apoptotic events as determined by DNA content after RNA interference (RNAi) transfection at 24 and 48 hours. Concatenation data gates were determined based on DNA content and dot-plots were generated from each sample per condition (n = 4).

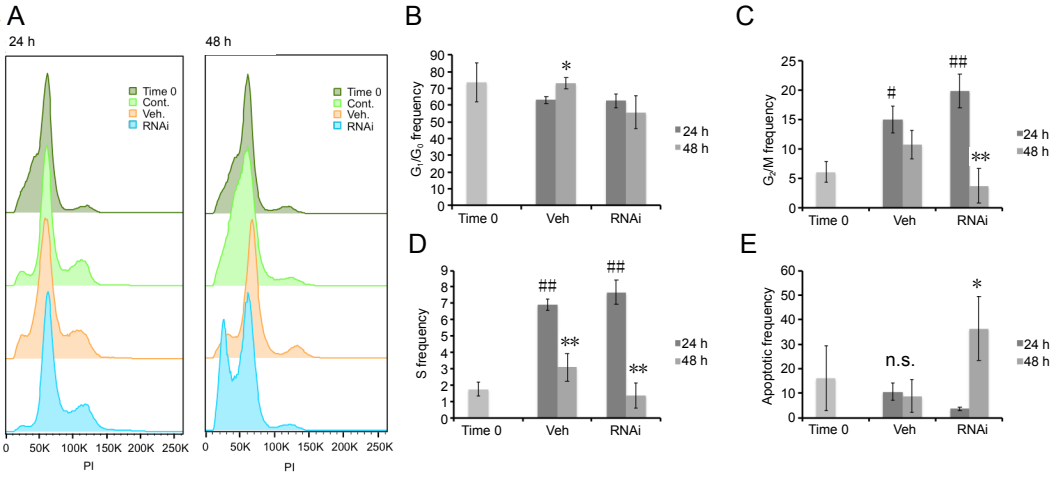

Figure 8 Analysis of apoptotic events within human cortical astrocytes labeled with propidium iodide.
(A) Concatenated data represent the overlay of all groups analyzed via flow cytometry: Control (lime), vehicle control (orange), and RNAi (blue), at 24 and 48 hours in comparison to cell cycle synchronization at Time 0 (green) revealed a dramatic shift in sub-2n population in the RNA interference (RNAi) condition at 48 hours, but not 24 hours relative to the other conditions. Quantitative data compares cell frequency across timepoints of each condition post release from cell cycle synchronization at G_1/G_0 (B), G_2/M (C) and S-phase (D). (E) Apoptotic events were defined by sub-2n events revealed an increase within the RNAi condition at 48 hours relative to 24 hours. Bar graph shows the mean ± SEM, n = 4 (∗P < 0.05, ∗∗P < 0.01, *vs.* 24 hours; #P < 0.05, ##P < 0.01, *vs.* time 0; unpaired t-test). PI: Propidium iodide.

Pucci B, Kasten M, Giordano A (2000) Cell cycle and apoptosis. Neoplasia 2:291-299.
Rapanelli M, Frick LR, Zanutto BS (2011) Learning an operant conditioning task differentially induces gliogenesis in the medial prefrontal cortex and neurogenesis in the hippocampus. PLoS One 6:e14713.
Riccardi C, Nicoletti I (2006) Analysis of apoptosis by propidium iodide staining and flow cytometry. Nat Protoc 1:1458-1461.
Rieger AM, Nelson KL, Konowalchuk JD, Barreda DR (2011) Modified annexin V/propidium iodide apoptosis assay for accurate assessment of cell death. J Vis Exp doi: 10.3791/2597.
Satyanarayana A, Kaldis P (2009) A dual role of Cdk2 in DNA damage response. Cell Div 4:9.
Siegenthaler JA, Miller MW (2005) Transforming growth factor beta 1 promotes cell cycle exit through the cyclin-dependent kinase inhibitor p21 in the developing cerebral cortex. J Neurosci 25:8627-8636.
Slee EA, Adrain C, Martin SJ (2001) Executioner caspase-3, -6, and -7 perform distinct, non-redundant roles during the demolition phase of apoptosis. J Biol Chem 276:7320-7326.
Spencer SL, Cappell SD, Tsai FC, Overton KW, Wang CL, Meyer T (2013) The proliferation-quiescence decision is controlled by a bifurcation in CDK2 activity at mitotic exit. Cell 155:369-383.
Surgucheva I, Newell KL, Burns J, Surguchov A (2014) New α- and γ-synuclein immunopathological lesions in human brain. Acta Neuropathol Commun 2:132.
Surgucheva I, Surguchov A (2008) Gamma-synuclein: cell-type-specific promoter activity and binding to transcription factors. J Mol Neurosci 35:267-271.
Ui-Tei K, Naito Y, Zenno S, Nishi K, Yamato K, Takahashi F, Juni A, Saigo K (2008) Functional dissection of siRNA sequence by systematic DNA substitution: modified siRNA with a DNA seed arm is a powerful tool for mammalian gene silencing with significantly reduced off-target effect. Nucleic Acids Res 36:2136-2151.
Ui-Tei K, Naito Y, Takahashi F, Haraguchi T, Ohki-Hamazaki H, Juni A, Ueda R, Saigo K (2004) Guidelines for the selection of highly effective siRNA sequences for mammalian and chick RNA interference. Nucleic Acids Res 32:936-948.
Ui-Tei K, Naito Y, Saigo K (2006) Essential notes regarding the design of functional siRNAs for efficient mammalian RNAi. J Biomed Biotechnol 2006:65052.
Welburn JP, Tucker JA, Johnson T, Lindert L, Morgan M, Willis A, Noble ME, Endicott JA (2007) How tyrosine 15 phosphorylation inhibits the activity of cyclin-dependent kinase 2-cyclin A. J Biol Chem 282:3173-3181.
Winham CL, Le T, Jellison ER, Silver AC, Levesque AA, Koob AO (2019) γ-Synuclein induces human cortical astrocyte proliferation and subsequent BDNF expression and release. Neuroscience 410:41-54.
Wu K, Weng Z, Tao Q, Lin G, Wu X, Qian H, Zhang Y, Ding X, Jiang Y, Shi YE (2003) Stage-specific expression of breast cancer-specific gene γ-synuclein. Cancer Epidemiol Biomarkers Prev 12:920-925.
Xia J, Chen SF, Lv YP, Lu LN, Hu WX, Zhou YL (2015) ZGDHu-1 induces G_2/M phase arrest and apoptosis in Kasumi-1 cells. Mol Med Rep 11:3398-3404.
Zhu M, Zhang B, Weng Z, Krishna R, Miao S, Lu Y, Wu K, Shi YE (2014) Synuclein γ compromises spindle assembly checkpoint and renders resistance to antimicrotubule drugs. Mol Cancer Ther 13:699-713. Mar;13(3):699-713.

P-Reviewers: Cartarozzi LP, Bufa AM; C-Editors: Zhao M, Li CH; T-Editor: Jia Y